ARTICLE OPEN

Check for updates

Choroid plexus volume is enlarged in long COVID and associated with cognitive and brain changes

Maria Diez-Cirarda[1]✉, Miguel Yus-Fuertes[2], Cristina Delgado-Alonso[1], Lidia Gil-Martínez[2], Carlos Jiménez-García[3], Maria José Gil-Moreno[1], Natividad Gómez-Ruiz[2], Silvia Oliver-Mas[1], Carmen Polidura[2], Manuela Jorquera[2], Ulises Gómez-Pinedo[1], Juan Arrazola[2], Silvia Sánchez-Ramón[3], Jorge Matias-Guiu[1], Gabriel Gonzalez-Escamilla[4,5] and Jordi A. Matias-Guiu[1,5]✉

Patients with post-COVID condition (PCC) present with diverse symptoms which persist at long-term after SARS-CoV-2 infection. Among these symptoms, cognitive impairment is one of the most prevalent and has been related to brain structural and functional changes. The underlying mechanisms of these cognitive and brain alterations remain elusive but neuroinflammation and immune mechanisms have been majorly considered. In this sense, the choroid plexus (ChP) volume has been proposed as a marker of neuroinflammation in immune-mediated conditions and the ChP epithelium has been found particularly susceptible to the effects of SARS-CoV-2. The objective was to investigate the ChP in PCC and evaluate its relationships with cognition, brain, and immunological alterations. One-hundred and twenty-nine patients with PCC after a mean of 14.79 ± 7.17 months of evolution since the infection and 36 healthy controls were recruited. Participants underwent a neuropsychological, and neuroimaging assessment and immunological markers evaluation. Results revealed ChP volume enlargement in PCC compared to healthy controls. The ChP enlargement was associated with cognitive dysfunction, grey matter volume reduction in frontal and subcortical areas, white matter integrity and diffusivity changes and functional connectivity changes. These ChP changes were also related to intermediate monocytes levels. Findings suggest that the ChP integrity may play a relevant role in the pathophysiology of cognitive deficits and the observed brain changes in PCC. The previously documented function of the ChP in maintaining brain homeostasis and regulating the entry of immune cells into the brain supports the presence of neuroinflammatory mechanisms in this disorder.

Molecular Psychiatry (2025) 30:2821–2830; https://doi.org/10.1038/s41380-024-02886-x

INTRODUCTION

Post-COVID condition (PCC) occurs in individuals with history of SARS-CoV-2 infection, in which a wide range of symptoms persist over more than 3 months after infection [1]. Symptoms related to PCC range from fatigue, anosmia, and dyspnea among others, and cognitive impairment has shown high prevalence [2–4]. These symptoms may persist over one year since the infection [5] and literature has shown a relationship between these cognitive deficits and reduced quality of life in PCC patients [6]. Cognitive impairment in PCC has been associated with brain changes [7], including reduced grey matter (GM) volume mostly located in orbitofrontal, temporal, hippocampal and cerebellar areas [8–11] and these changes might be accompanied by white matter (WM) changes [12, 13] and functional connectivity (FC) changes [14].

Unfortunately, the underlying mechanisms of symptoms persistence and related brain changes remain elusive. The firstly proposed direct effect of the SARS-CoV-2 through its entrance in the central nervous system by olfactory fibers or nasal passages seems to be uncommon. Further, the effects of acute hypoxia could only account for symptoms in the most severe cases, because cognitive symptoms after COVID-19 are also evident in patients with mild acute infections. Consequently, there is a recent interest on the role of neuroinflammation and immune mechanisms in understanding the neurological consequences of the virus [15–17].

The choroid plexus (ChP) is located inside the ventricular system of the brain. The main function of the ChP is producing cerebrospinal fluid (CSF) and its clearance, maintaining the homeostasis of CSF [18]. The ChP is in charge of secretory, transport and barrier functions between the blood and extracellular fluid and the central nervous system, forming the blood-CSF barrier. Because of its main role in transport of molecules into the central nervous system, the ChP has the role of neuroimmune regulation, and has been considered the gateway of inflammatory cells into the brain [19]. Moreover, ChP blood-CSF barrier is more permeable than the tightly regulated blood-brain barrier and, thus, may potentially be the site for SARS-CoV-2 entry into the brain. In addition, dysregulation of the blood-brain barrier has been recently suggested as a relevant mechanism in the pathophysiology of brain fog after COVID-19 [20].

[1]Department of Neurology, Hospital Universitario Clínico San Carlos. Health Research Institute "San Carlos" (IdISCC). Universidad Complutense de Madrid, Madrid, Spain. [2]Department of Radiology, Hospital Universitario Clinico San Carlos. Health Research Institute "San Carlos" (IdISCC). Universidad Complutense de Madrid, Madrid, Spain. [3]Department of Immunology, Hospital Universitario Clínico San Carlos. Health Research Institute "San Carlos" (IdISCC). Universidad Complutense de Madrid, Madrid, Spain. [4]Department of Neurology, Focus Program Translational Neuroscience (FTN), University Medical Center of the Johannes Gutenberg, University Mainz, Mainz, Germany. [5]These authors contributed equally: Gabriel Gonzalez-Escamilla, Jordi A. Matias-Guiu. ✉email: mdcirarda@salud.madrid.org; jordi.matias-guiu@salud.madrid.org

Received: 29 March 2024 Revised: 9 December 2024 Accepted: 31 December 2024
Published online: 15 January 2025

Studies on organoids have revealed that the entry factors ACE2 and TMPRSS2 of SARS-CoV-2 are expressed in ChP cells. Additionally, these studies suggest that SARS-CoV-2 infection causes damage to the ChP epithelium, making it a central nervous system structure particularly susceptible to the effects of the virus [21, 22]. Simultaneously, transcriptomic analysis of patients who died due to severe COVID-19 has demonstrated inflammation and dysregulation in the ChP, which was associated with neuroinflammation in the frontal cortex [23].

Neuroimaging analysis is a useful approach to evaluate the ChP in vivo. Neuroimaging studies in other diseases revealed increased ChP volume in multiple sclerosis related to disease severity and neuroinflammation [24, 25], but also in frontotemporal dementia [26]. A recent study revealed increased ChP volume in subacute COVID-19 patients [27]. However, to our knowledge, no studies have analyzed the ChP in patients with PCC. The study of ChP in PCC may help unraveling the underlying mechanisms of brain changes in these patients, because of the key role of ChP in regulating the access of neuroinflammatory cells to the central nervous system.

Therefore, the aim of the present study was threefold: 1) To evaluate the ChP integrity in PCC patients; 2) To investigate the relationships between ChP volume and cognitive characteristics, as well as structural and functional brain changes; 3) To assess the immunological alterations related to ChP volume changes, in order to provide complementary infection-related molecular information.

SUBJECTS AND METHODS

Participants

One-hundred and twenty-nine participants with PCC were recruited at the Hospital Clínico San Carlos from November 2020 to July 2022. These patients were enrolled after 14.79 ± 7.17 months from the acute infection.

PCC patients were enrolled in the study if they had: 1) Diagnosis of COVID-19 confirmed by RT-PCR at least three months before the inclusion in the study; 2) Cognitive complaints temporally-related to the SARS-CoV-2 infection. Exclusion criteria for PCC patients included: 1) Presence of cognitive complaints before COVID-19; 2) Traumatic brain injury, neurological disorder, or/and active psychiatric disorder potentially associated with cognitive impairment; 3) History of abuse of alcohol or other toxics; 5) Any condition associated with cognitive impairment at the time of the assessment such as drugs, uncontrolled medical conditions; 6) Sensory disorder potentially biasing cognitive assessments; 7) Deep WM cerebral small vessel disease (Fazekas grade 2 or higher).

Additionally, a healthy control group (HC; $n = 36$) was recruited. HC participants were excluded if: 1) History of SARS-CoV-2 infection evaluated through a serological analysis; 2) Presence of cognitive impairment or complaints; 3) History of any neurological or psychiatric disorder potentially associated with cognitive impairment; 4) History of abuse of alcohol or other toxics; 5) Any condition associated with cognitive impairment at the time of the assessment such as drugs, uncontrolled medical conditions; 6) Sensory disorder potentially biasing cognitive assessments; 7) Deep WM cerebral small vessel disease (Fazekas grade 2 or higher).

Neuropsychological and clinical assessment

A trained neuropsychologist conducted the cognitive and clinical assessment, which included the evaluation of attention, working memory, processing speed, executive functions, memory, language, and visuoperceptive and visuospatial abilities. Clinical assessment included fatigue, anxiety, depression, olfactory and sleep disturbances. Specific tests can be found in Supplementary Materials.

Neuroimaging acquisition

Patients were scanned using a 3.0 T Magnet (GE Signa Architect) and a 48-channel head coil. T1-weighted images, diffusion-weighted images, and resting-state fMRI were acquired in a single session. Neuroimaging acquisition parameters can be found in Supplementary Materials.

Choroid plexus segmentation

A Gaussian Mixture Model was applied to segment the ChP within the lateral ventricles [28]. Firstly, FreeSurfer (https://surfer.nmr.mgh.harvard.edu/) segmentation is applied to obtain masks including the ChP, ventricular walls, and CSF of the lateral ventricles. Then a Bayesian Gaussian Mixture Model with two components was applied to identify the highest-intensity voxels. Following a smoothing (sigma = 1 mm), a second Bayesian Gaussian Mixture Model with three components was applied to identify the highest intensity voxels, which were classified as ChP voxels. Each patient's ChP segmentation was visually inspected and overlaid on each patient's T1 image, by two researchers independently and reached consensus. Manual correction was performed in 61 ChP segmentations.

ChP volumes from right and left hemispheres were extracted and created a composite score representing the mean bilateral ChP volume (mm^3), which was used for subsequent analyses.

T1-weighted images

T1-weighted images were preprocessed and analysed for voxel-based morphometry analysis using the DARTEL procedure (Diffeomorphic Anatomical Registration Through Exponentiated Lie Algebra) in SPM12 [29]. After orientation and segmentation, the mean template was created, and then we performed spatial normalization into the Montreal Neurological Institute (MNI) template space. Images were modulated and smoothed with an isotropic Gaussian kernel of 8 mm full-width at half maximum (FWHM). Regression analyses were performed between ChP volume and GM volume, with age and Total Intracranial Volume (TIV) as covariates. Significance was set at cluster-level $p < 0.05$ FDR-corrected (two-sided). The AAL atlas parcellation was used. Moreover, a mask was created with the GM areas significantly associated with ChP volume, and mean GM volume values were extracted using MARSbar software (www.marsbar.sourceforge.net), and introduced in SPSS for correlation analyses with cognition.

Some specific subcortical structures anatomically related to the ChP (lateral ventricles, corpus callosum, and thalamus) were also segmented using Freesurfer software version v7.2.0 [30] following the Freesurfer's standard analysis pipeline [31, 32].

All surface models were visually inspected for accuracy. No model was excluded due to misclassification of tissue types. Subcortical volumes for left and right hemispheres were extracted based on the aseg atlas parcellation [33] and mean bilateral volumes were calculated.

Diffusion-weighted images

Diffusion data were preprocessed and analyzed in FMRIB Software Library (FSL) (v.6.0.5) [34]. First, each subject's images were concatenated and radiologically oriented. Then, *topup* was applied to estimate and correct susceptibility-induced distortions (fieldmap estimation) [35]. Then, BET brain extraction was applied [36]. *Eddy* command was used to correct for distortion (eddy currents, susceptibility-induced distortions, and subject's motion) [37] with a fieldmap estimated by *topup*. After, *dtifit* command was applied to fit diffusion tensors into the eddy-corrected data. For voxelwise statistical analyses, data were processed applying the standard FSL pipeline for Tract-Based Spatial Statistics (TBSS) [38].

Finally, fractional anisotropy (FA), mean diffusivity (MD), radial diffusivity (RD), and axial diffusivity (AD) whole-brain maps were calculated. Regression analyses were performed between ChP volume and FA, MD, RD, and AD maps, with age and TIV as covariates. *Randomise* was performed with 5000 permutations. Significance was set at $p < 0.05$ FWE-corrected (two-sided), $k > 50$. JHU-ICBM-DTI-81 WM Labels and JHU White-Matter tractography Atlas from FSL were used for anatomical localization of the results. Moreover, masks of significant WM regions associated with ChP volume were created, and mean WM index values were extracted for correlation analyses with cognition.

Resting-state fMRI

Functional connectivity (FC) analysis was performed using the CONN Functional Connectivity Toolbox 18.b [39]. After removing the first 5 scans, each subject' 200 functional images were realigned and unwarped, non-linear coregistered with structural data, slice timing corrected (interleaved bottom-up), spatially normalized into the standard MNI space (Montreal Neurological Institute), then, outliers were detected (ART-based scrubbing) and finally, images were smoothed using a Gaussian kernel of 8 mm FWMH. As recommended, band-pass filtering was performed with a frequency window of 0.008 to 0.09 Hz.

To correlate ChP volume with FC, a whole-brain Region of interest (ROI) ROI-to-ROI approach analysis was performed according to Conn toolbox options, with age as covariate. Significance was set at $p < 0.05$ FDR-corrected (two-sided). The Automated Anatomical Labeling atlas (AAL) atlas parcellation included in CONN toolbox was used for results localization. BrainNet Viewer software was used for FC visualization purposes [40]. Moreover, FC from regions showing significant associations with ChP volume were extracted and included in SPSS for correlation analysis with cognition. To do so, a composite score with FC values was created, and negative connectivity values were reversed.

Immunology analysis

Blood samples were collected in EDTA vacuum tubes from a subsample of the patients ($n = 38$) and a secondary healthy control group ($n = 14$) recruited for blood samples comparison, similar in age ($p = 0.467$), and sex ($p = 0.440$). Fresh blood samples were directly processed and analyzed. Peripheral blood cells were incubated with a mixture of CD14 APC-Cy7 (BD Pharmigen), CD16 FITC (Cytognos), CD11b (eBioscience), CD69 PE-Cy7 (BD Biosciences), CX3CR1 PerCP-Cy5.5 (Biolegend), CCR2 APC (BD Biosciences) and CCR5 BV421 (BD Horizon) antibodies during 20 min at RT after lysing solution was added for 15 min. Each sample was washed twice with PBS1x and pelleted by centrifugation 1200 rpm during 5 min. After the peripheral blood mononuclear cells were resuspended in 300 uL of FACS buffer and acquired in the cytometer. The monocytic population went under examination through multiparametric flow cytometry utilizing the FACS Canto II (BD Biosciences, San José, CA) and samples were measured and analyzed using BD FACSDiva software (BD Biosciences). For the gating strategy, we selected the monocytic population based on the complexity and size of the cell (SSC-H vs FSC-H), then only single cells (FSC-A vs FSC-H) were considered for the gating based on the immunoprophile. At least 200000 events were measured in each sample. Intermediate monocytes ($CD14^{+}CD16^{+}$) were analyzed based on their previous association with pro-inflammatory factors [41].

Moderation analysis

Due to the known role of ChP forming the blood-CSF barrier, and given the well-established relationship between GM volume and cognition, we aimed to investigate whether the ChP volume could be a moderator on the relationship between GM volume and cognitive impairment.

Thus, we created a cognitive composite score (CS Cognition), with the cognitive domains that showed more accentuated impairment in PCC patients (attention, working memory, processing speed, and executive functions), with the following tests: Span Forward, Span Backward, SDMT and Stroop test (W, C, W-C).

Moderation analysis was performed with Model 1 PROCESS v4.2 for SPSS [42] and included CS Cognition as dependent variable, GM volume as independent variable, and ChP volume as moderator variable. Age and TIV were included as covariates. All variables were demeaned. Then, Johnson–Neyman technique was applied to identify the cut-off score indicating the region of significance. That is, Johnson–Neyman technique helps identifying the value of the moderator, in this case the ChP volume, for which the effect of GM volume over CS Cognition changed from statistically non-significant to significant. Boostrapping was applied (5000 samples) and confidence interval was set at 95% with $p < 0.05$. Finally, ChP subgroup analyses were performed to test differences between those patients with a ChP volume under the cut-off of significance (ChP-small) ($n = 61$), compared to those PCC patients which ChP volume was higher than the cut-off score (ChP-large) ($n = 68$).

Statistical analysis

Statistical analyses were conducted using IBM SPSS Statistics for Windows, version 26.0 (IBM Corp., Armonk, NY: IBM Corp) [43]. Sociodemographic, clinical, and cognitive differences between groups were calculated using *T*-test or ANOVA and Chi-squared tests for categorical data. Comparisons between PCC and HC included age and TIV as covariates. Neuroimaging analyses regarding correlations between ChP volume and GM, WM, or FC indexes, included age and TIV as nuisance covariates, and all neuroimaging analyses were corrected for multiple comparisons. Correlation analyses were performed with partial correlation coefficient estimation using age and TIV as covariates and set at $p < 0.05$ (two-sided). Regarding correlations with cognition, Bonferroni correction was also indicated, corrected by the total number of cognitive tests, at $p < 0.0017$. Correlations were interpreted small, moderate, and large when scores were 0.10, 0.30, and 0.50, respectively [44]. Moderation analyses also included age and TIV as covariates. Finally, ChP subgroup analyses were performed. Cognitive, brain, and immunological differences between ChP-small and ChP-large subgroups were performed with age, sex, and TIV as covariates.

Ethics statement

The present study was approved by the ethics committee from Hospital Clínico San Carlos (reference: 21/062-E) and participants provided written informed consent prior to research participation. Research was conducted following the principles of the Declaration of Helsinki and in accordance with local regulations.

RESULTS

Participants sociodemographics

PCC and HC shared similar sociodemographic characteristics (Table 1). PCC patients had a mean of 49.35 ± 10.29 years old, 73.64% were women, and a mean of 14.79 ± 7.17 months of evolution since infection. PCC patients presented abnormal cognitive function, especially in attention, processing speed, executive functions, and episodic memory. Moreover, 86.6% presented with fatigue, 84.5% with sleep disturbances, 49.6% referred anxiety symptoms, 26.4% referred depression symptoms, and 26.4% anosmia. Neuropsychological and clinical results can be found in Supplementary Tables S1 and S2.

ChP volume and associations with cognitive and clinical symptoms in PCC

PCC patients had increased mean ChP volume compared to HC [PCC: mean ± SD = 796.21 ± 93.10; HC: mean ± SD = 764.48 ± 189.49] ($F = 20.072$; $p < 0.001$) (see Fig. 1.A).

The increased ChP volume in PCC correlated negatively and significantly with cognition. That is, the larger the ChP volume, the poorer cognitive performance. Specifically, ChP volume showed significant relationships with Digit Span Backwards ($r = -0.233$; $p = 0.009$), Corsi Span Forwards ($r = -0.213$; $p = 0.018$), and ROCF Recognition ($r = -0.184$; $p = 0.041$).

On the contrary, ChP volume in PCC group showed no associations with clinical variables, such as fatigue (MFIS total: $p = 0.508$), anxiety (STAI: $p = 0.116$); depression (BDI: $p = 0.317$), olfaction (BSIT; $p = 0.930$), or sleep disturbances (PSQI; $p = 0.457$).

ChP volume associations with GM volume

ChP volume correlated significantly with bilateral ventricles volume ($r = 0.552$; $p < 0.001$), and inversely with corpus callosum volume ($r = -0.254$; $p = 0.004$) and thalamus volume ($r = -0.180$; $p = 0.043$).

Voxel-based morphometry results revealed a negative association between ChP volume and GM volume mostly in subcortical and prefrontal areas in PCC patients (Fig. 1B, C). ChP volume in PCC was significantly associated with reduced GM volume in the inferior and middle orbitofrontal cortex, frontal inferior and Rolandic operculum, insula, cingulum, caudate, putamen,

Table 1. Sociodemographic and clinical characteristics.

	HC ($n = 36$)	PCC ($n = 129$)	*p*
Age (years)	49.33 (15.99)	49.35 (10.29)	.996
Sex (Women) (*n*,%)	22 (61.11%)	95 (73.64%)	.152
Education (years)	15.43 (3.28)	14.97 (3.62)	.587
Evolution (months)	–	14.79 ± 7.17	–
Hospital Admission (*n*,%)	–	36 (27.90%)	–
Hypertension (*n*,%)	–	33 (25.58%)	–
Diabetes (*n*,%)	–	13 (10.07%)	–
Dyslipidemia (*n*,%)	–	31 (24.03%)	–

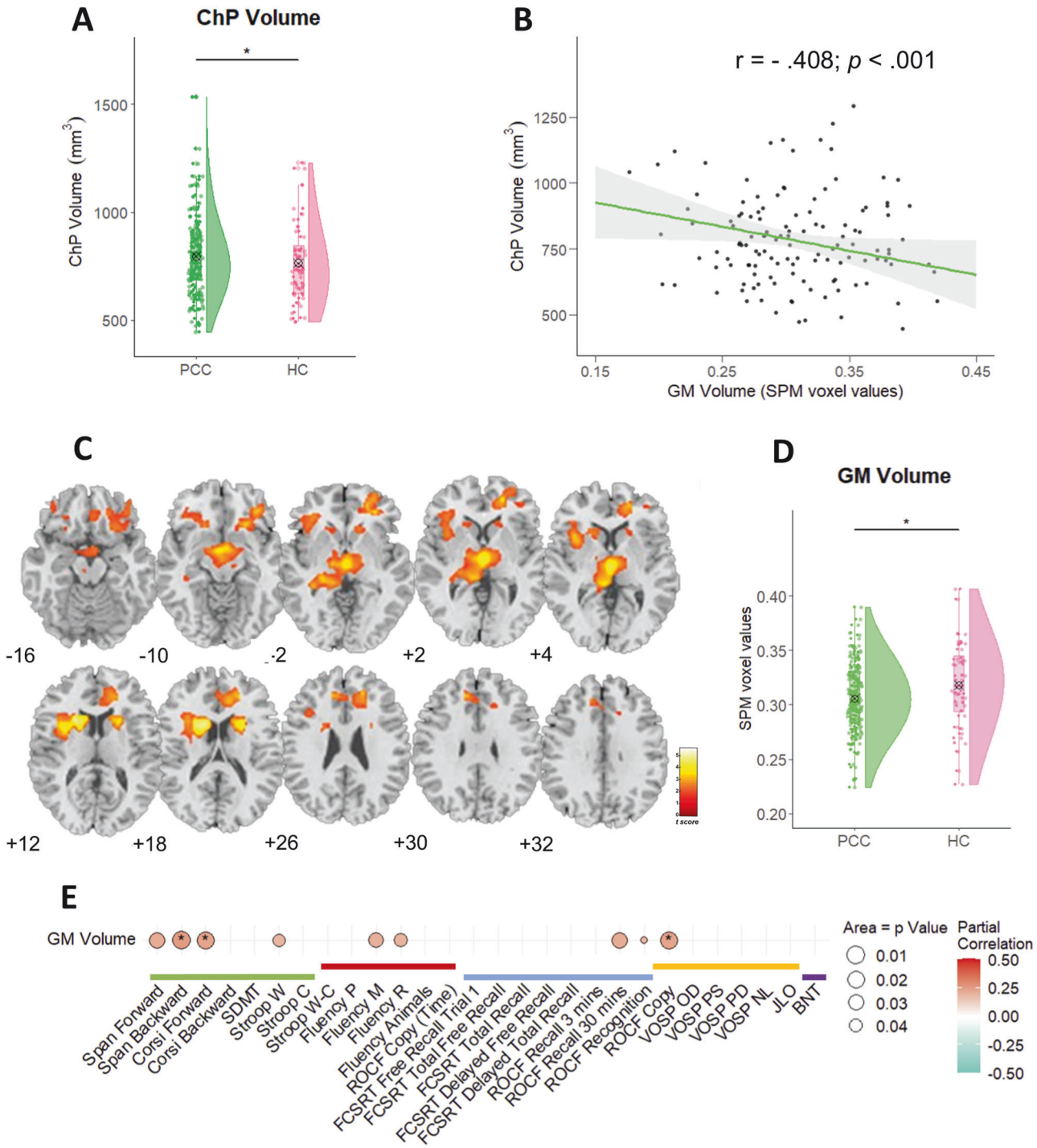

Fig. 1 ChP volume and associations with GM volume. A Significant differences in ChP volume (mm^3) between groups. Crossed circle indicates the mean; **B** Correlation between GM volume and ChP volume in PCC; **C** Visual representation of GM volume associations with ChP volume in PCC patients; **D** Significant differences in GM volume between groups. Crossed circle indicates the mean; **E** GM volume correlations with cognition. * $p = <0.01$. Green line = Attention and Working Memory; Red line = Executive Functions; Blue line = Learning and Memory; Orange line = Visuospatial and visuoconstructive ability; Purple line = Language.

pallidum, thalamus, and hippocampus ($p < 0.05$ FWE-corrected) (Supplementary Table S3). A GM mask with these results was created, and GM volume differences between groups were evaluated, showing that PCC had reduced GM volume compared to HC (PCC vs HC: $F = 33.537$; $p < 0.001$) (Fig. 1D).

Moreover, correlations were performed between the GM volume (within the GM mask), and cognition. Results revealed significant positive associations with attention, working memory, executive functions, memory, and visuoconstructive abilities ($p < 0.05$) (see Fig. 1E).

ChP associations with white matter integrity

ChP volume was associated significantly with WM integrity and diffusivity in PCC patients, mostly in WM tracts located near the

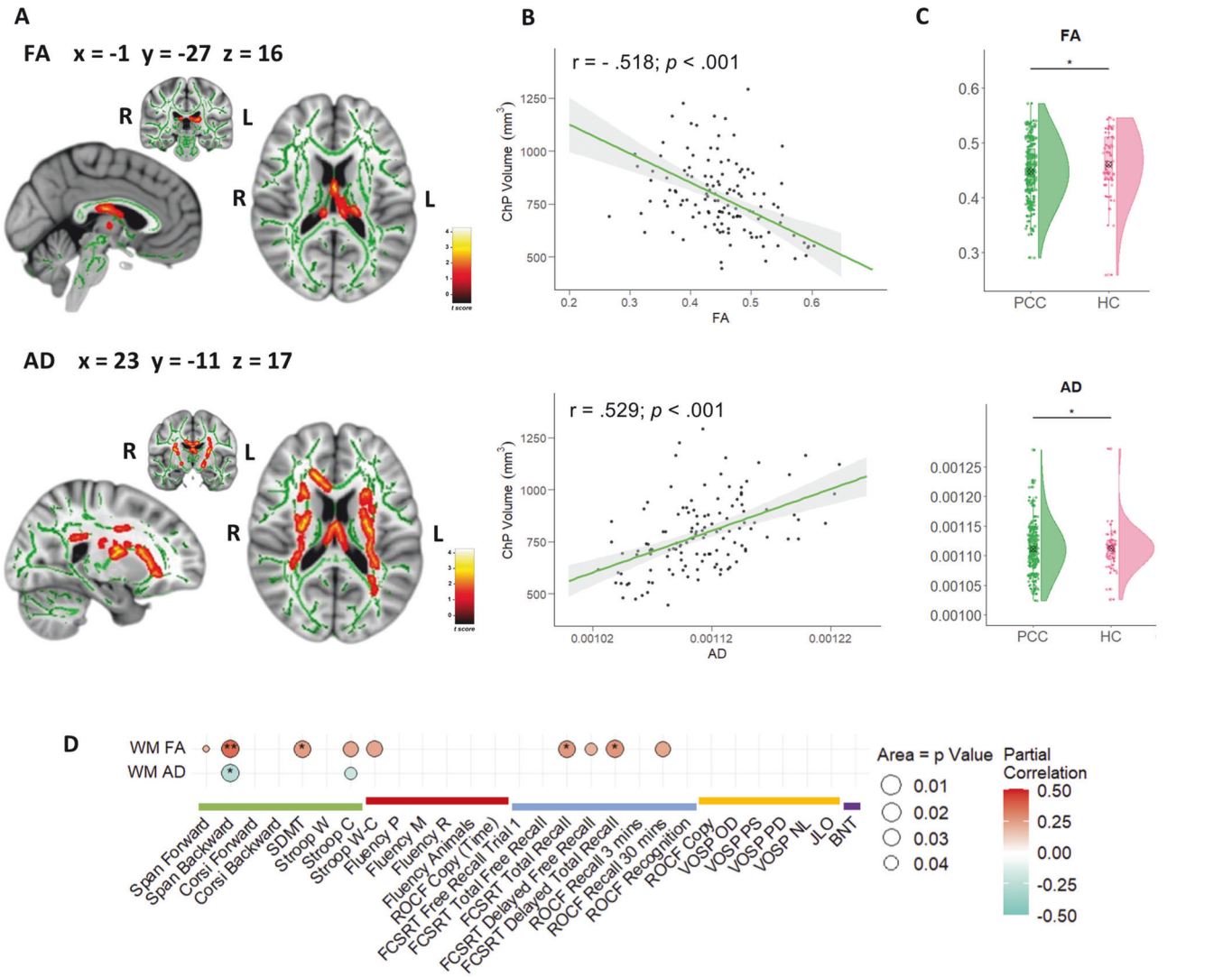

Fig. 2 ChP volume associations with white matter FA and AD. A Visual representation of white matter correlates of ChP volume; **B** Correlation between WM indexes and ChP Volume in PCC; **C** FA, and AD values distribution in each group and significant differences. Crossed circle indicates the mean; **D** WM FA and AD correlations with cognition. * $p = <0.01$; ** $p < 0.0017$ (Bonferroni corrected). FA = Fractional Anisotropy; AD = Axial Diffusivity; FC = Functional Connectivity. Green line = Attention and Working Memory; Red line = Executive Functions; Blue line = Learning and Memory; Orange line = Visuospatial and visuoconstructive ability; Purple line = Language.

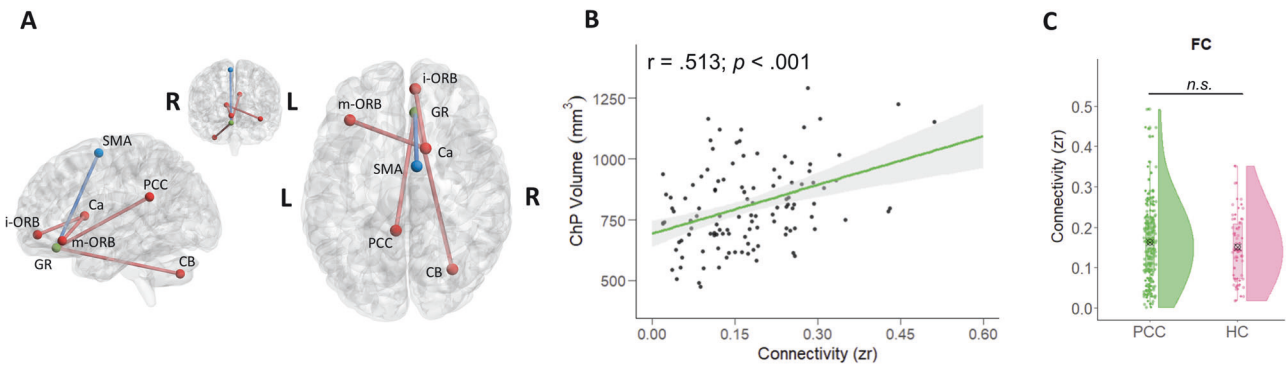

Fig. 3 ChP volume associations with FC. A Visual representation of functional connectivity correlates of ChP volume (Red = positive correlation; Blue = Negative correlation); **B** Correlation between FC and ChP Volume in PCC; **C** FC values distribution in each group. Crossed circle indicates the mean (n.s. = non-significant). SMA = Somatomotor area; PCC = Posterior Cingulate Cortex; i-ORB = Inferior Orbitofrontal; CB = Cerebellar; GR = Gyrus Rectus; Ca = Caudate; m-ORB = Middle Orbitofrontal; FC = Functional Connectivity.

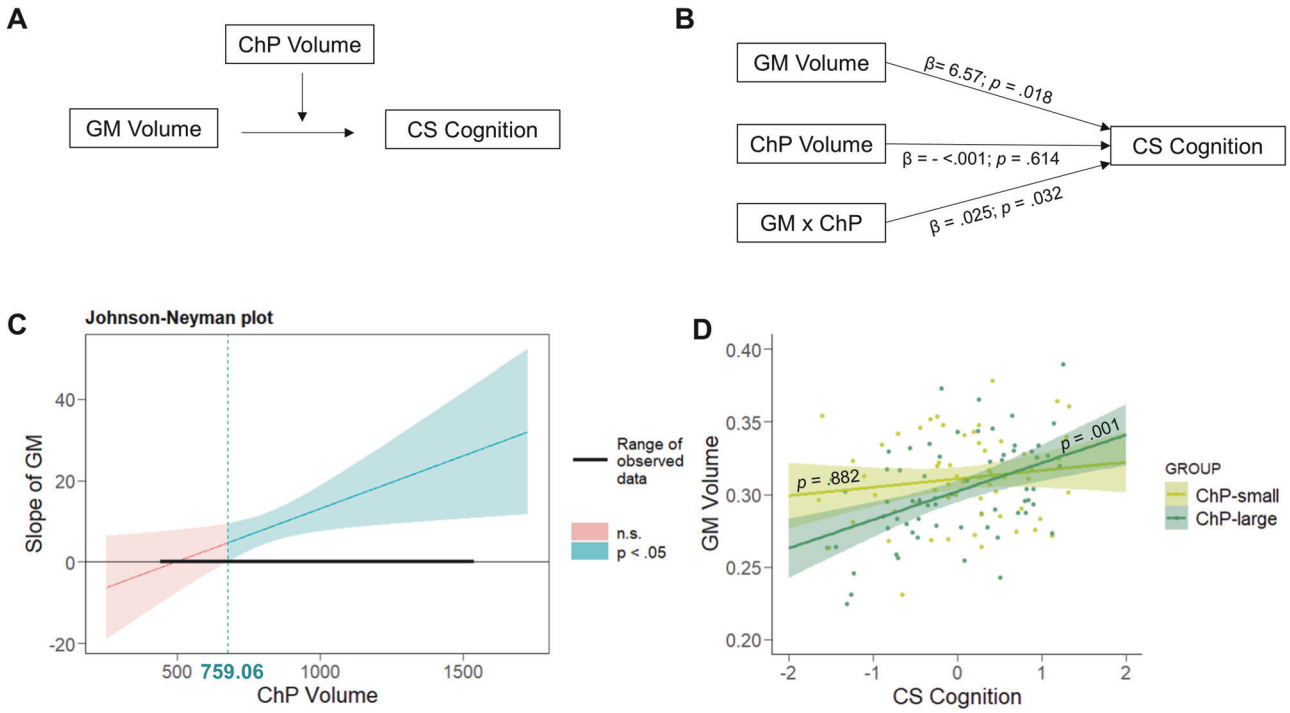

Fig. 4 ChP volume moderation between GM volume and cognition in PCC. A Proposed moderation model; **B** Statistical diagram with the effects of GM Volume, ChP volume and the interaction between variables on CS Cognition; **C** Graphical representation of the Johnson-Neyman method and cut-off score for significance; **D** Association between GM volume and cognition for both subgroups (ChP-small and ChP-large).

ChP, and tracts connecting with frontal areas. ChP volume correlated with reduced FA and increased AD values in bilateral fornix, bilateral anterior thalamic radiation, and callosal body, and with increased AD in inferior fronto-occipital fasciculus and middle longitudinal fasciculus ($p < 0.05$ FWE-corrected) (Fig. 2A, B, Supplementary Table S4). No significant relationships were found with MD or RD.

FA and AD values were extracted from those areas showing significant associations with ChP volume. Figure 2C presents FA and AD values distribution in each group. FA values were significantly reduced in PCC compared to HC ($F = 13.291$; $p < 0.001$). Regarding AD, PCC showed significant differences with HC ($F = 6.151$; $p < 0.001$).

Moreover, WM FA and AD values correlated significantly with cognition. Specifically, FA was positively associated with attention, working memory, processing speed, executive functions, and memory ($p < 0.05$), while WM AD was negatively associated with attention and working memory (see Fig. 2D).

ChP volume associations with functional connectivity

ChP volume correlated significant with FC in PCC patients (Fig. 3A). Specifically, increased ChP volume was associated with increased FC between right caudate and right medial orbitofrontal area ($t = 3.93$; $p = 0.015$ FDR-corrected) and right inferior orbitofrontal area ($t = 3.41$; $p = 0.04$ FDR-corrected). In addition, ChP volume correlated with increased FC between the gyrus rectus with left posterior cingulum ($t = 3.42$; $p = 0.04$ FDR-corrected) and right cerebellar Crus II ($t = 3.31$; $p = 0.04$ FDR-corrected). ChP volume also showed inverse correlations between the gyrus rectus and somatomotor area ($t = -3.54$; $p = 0.04$ FDR-corrected). FC values were extracted and created a composite score, which correlated with ChP volume ($r = 0.396$; $p < 0.001$) (see Fig. 3B).

Figure 3C presents FC values distribution in each group. FC values between these nodes did not show significant differences between PCC and HC groups.

Moreover, correlations were performed between the FC values and cognition, but no significant correlations were found.

ChP associations with immunology

Following immunological profiling of the myeloid population in the peripheral blood, we found an inverse correlation between the ChP volume and the expression of $CD11b^{+}$ ($r = -0.344$; $p = 0.040$), along with a positive correlation with the expression of CX3CR1 ($r = 0.350$; $p = 0.036$). Moreover, PCC patients presented diminished proportion of $CD14^{+}CD16^{+}$ monocytes ($F = 4.301$; $p = 0.019$), concomitant with reduced proportion of CCR2 compared to HC ($F = 6.391$; $p = 0.003$).

ChP volume as a moderator between GM volume and cognition in PCC

We found a significant moderation effect of ChP volume on the relationship between GM volume (within the GM mask) and cognitive performance in PCC. A graphical representation of the model is shown in Fig. 4A.

The interaction between GM volume and ChP volume showed a significant effect on CS Cognition ($\beta = 0.025$; $t = 2.16$; $p = 0.032$). In addition, GM volume showed a significant effect on CS Cognition ($\beta = 6.577$; $t = 2.39$; $p = 0.018$), while ChP volume effect on CS Cognition was not significant ($\beta = -<0.001$, $t = -0.50$; $p = 0.614$) (Fig. 4B).

Figure 4C visualizes the Johnson-Neyman plot. The continuous line showed the conditional effect of GM volume on cognition depending on the ChP volume. The moderation of ChP volume on the relationship between GM volume and cognition transitioned from not significant to statistically significant when ChP volume was ≥ 759.06 mm^3.

PCC group was divided in two subgroups, ChP-small and ChP-large, based on the cut-off established. Finally, for visualization purposes, the association between GM volume and CS Cognition is represented for both subgroups ChP-small and ChP-large

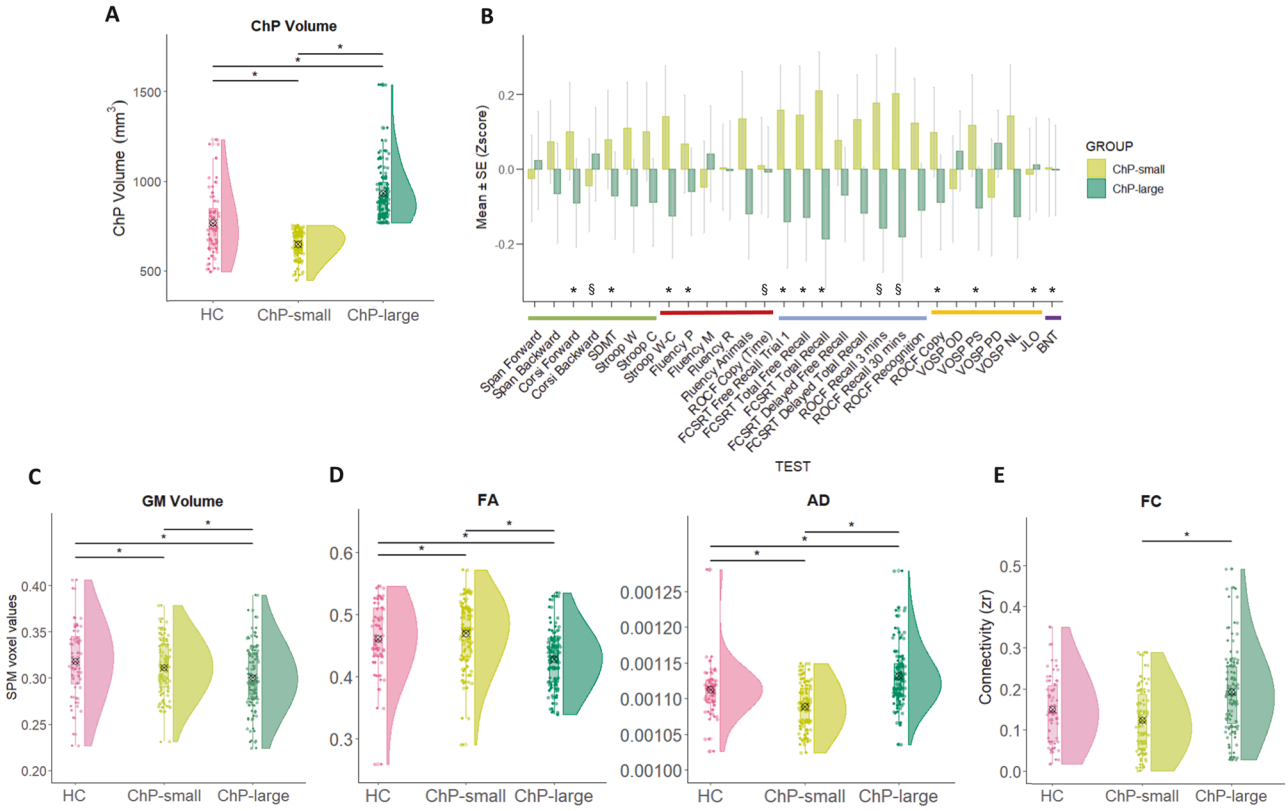

Fig. 5 ChP subgroups differences. A Differences in ChP volume between groups; **B** Mean and standard error (Z-scores) of cognitive performance in ChP-small and ChP-large subgroups; * $p < 0.05$; § $p < 0.0017$. SE = Standard Error; ROCF = Rey-Osterrieth Complex Figure; SDMT = Symbol Digit Modalities Test; FCSRT = Free and Cued Selective Reminding Test; VOSP = Visual Object and Space Perception Battery; JLO = Judgment Line Orientation; BNT = Boston Naming Test. Green line = Attention and Working Memory; Red line = Executive Functions; Blue line = Learning and Memory; Orange line = Visuospatial and visuoconstructive ability; Purple line = Language; **C** Differences in GM volume between groups; **D** Differences in WM indexes between groups; **E** Differences in FC between groups.

(Fig. 4D). Correlation between GM volume and CS Cognition was only significant for ChP-large subgroup ($r = 0.388$; $p = 0.001$) but showed no significant relationships for the ChP-small subgroup ($r = 0.020$; $p = 0.882$).

ChP subgroup differences

We further aimed to investigate differences in clinical or brain characteristics between subgroups. ChP-small and ChP-large subgroups showed significant differences in age and sex, showing ChP-small subgroup younger participants and increased number of women ($p < 0.05$). Moreover, ChP-large subgroup had increased percentage of patients with hypertension ($p < 0.05$) (Supplementary Table S5).

As expected, ChP volumes between HC, ChP-small, and ChP-large showed significant differences ($F = 33.686$; $p < 0.001$). ChP-small subgroup [mean ± SD = 646.47 ± 78.68] showed reduced ChP volume as compared to ChP-large subgroup [mean ± SD = 930.54 ± 164.21] ($F = 43.118$; $p < 0.001$), and both subgroups showed significant differences compared to HC [mean (SD) = 764.48 ± 189.49] (HC vs ChP-small: $F = 12.760$; $p < 0.001$; HC vs ChP-large: $F = 11.937$; $p < 0.001$) (Fig. 5A).

Regarding cognition, ChP-large subgroup showed increased cognitive impairment compared to ChP-small subgroup across most of the cognitive domains (see Fig. 5B) but no significant differences were found in clinical symptoms.

Regarding GM volume, ANOVA analysis revealed significant differences between HC, ChP-small, and ChP-large subgroups ($F = 24.713$; $p < 0.001$). Particularly, ChP-large and ChP-small subgroups showed reduced GM volume compared to HC (ChP-large vs HC: $F = 18.842$; $p < 0.001$; ChP-small vs HC: $F = 11.751$; $p < 0.001$). Interestingly, ChP-large subgroup also showed reduced GM volume compared to ChP-small subgroup ($F = 35.850$; $p < 0.001$) (Fig. 5C).

Regarding WM integrity and diffusivity, significant differences were found between HC, ChP-large, and ChP-small in WM FA ($F = 11.545$; $p < 0.001$). ChP-large showed reduced FA compared to HC ($F = 11.004$; $p < 0.001$) and compared to ChP-small ($F = 10.738$; $p < 0.001$). On the contrary, ChP-small showed increased FA compared to HC ($F = 4.755$; $p = 0.002$). Regarding WM AD, comparisons between HC, ChP-large, and ChP-small were also significant ($F = 9.549$; $p < 0.001$). ChP-large revealed increased AD compared to HC ($F = 4.602$; $p = 0.002$), and compared to ChP-small ($F = 11.517$; $p < 0.001$). On the contrary, ChP-small showed reduced AD compared to HC ($F = 3.237$; $p = 0.016$) (Fig. 5D).

Focusing on FC, results revealed significant differences when comparing HC, ChP-small, and ChP-large ($F = 5.282$; $p < .001$), specifically, ChP-small revealed reduced connectivity compared to ChP-large ($F = 6.995$; $p < 0.001$) (Fig. 5E).

Finally, subgroup analysis of the $CD14^{+}CD16^{+}$ monocytes between individuals with ChP-small and ChP-large revealed significant differences. The ChP-large subgroup presented lower proportion of $CD11b^{+}$ within the population ($F = 3.128$; $p = 0.028$), as well as reduced proportion of CCR5 ($F = 2.751$; $p = 0.044$) but increased expression of CD69 ($F = 3.601$; $p = 0.015$) compared to ChP-small.

Further analyses were performed to test the influence of premorbid risk factors in cognition and brain of PCC patients. ChP-large subgroup showed increased percentage of hypertension compared to the ChP-small subgroup. We found that patients from the ChP-large subgroup with hypertension presented with

increased alterations in GM volume, white matter integrity and diffusivity and poorer cognition compared to those patients from the ChP-large subgroup without hypertension ($p < 0.05$).

DISCUSSION

The present study provides novel evidence regarding the involvement of ChP in patients with post-COVID conditions. Importantly, ChP volume enlargement was associated with brain GM volume reduction and cognitive dysfunction, revealing a moderator role of the ChP volume between GM volume and cognition. Furthermore, ChP volume increment was associated with WM integrity and diffusivity alterations, increased functional connectivity, and immunological markers changes in PCC patients.

We found increased ChP volume in PCC patients compared to HC with similar sociodemographic characteristics. Interestingly, the increased ChP volume was associated with cognitive dysfunction, showing those patients with higher ChP volume to have greater cognitive impairment compared to those patients with smaller ChP volume. The current results are well in line with recent findings in other disorders, such as multiple sclerosis, in which enlarged ChP tightly related to neuroinflammation [25], as well as disease severity and cognitive dysfunction [24]. ChP enlargement has also been detected in neurodegenerative disorders, especially in frontotemporal dementia [26], and Alzheimer's disease [45].

The increased ChP volume was associated with reduced GM volume in regions closely located to the ChP, such as the corpus callosum, thalamus, and basal ganglia, but also with reduced GM volume in the insula, cingulum, hippocampus, and frontal and orbitofrontal cortices. These brain GM abnormalities were in turn associated with cognitive deficits, mostly with attention, executive functions, and episodic memory. Together, suggesting a tight relationship between the ChP and brain integrity. Previous studies in PCC also found brain GM volume reduction in similar areas, which were linked to cognitive dysfunction [10, 11, 46]. Interestingly, the ChP volume was related to reduced hippocampal volume, and the hippocampus has been found a structure susceptible to injuries caused by SARS-CoV-2 infection [47], particularly the dentate gyrus, both in vivo and in post-mortem samples [48]. The ChP-CSF system has been found to have a role in brain neurogenesis, due to the influence of CSF in the dentate zone of the hippocampus and the proximity to the subventricular zone [18].

The ChP volume did not exhibit significant associations with some of the symptoms commonly reported on PCC patients, including fatigue, anxiety, depression, sleep disturbances, or olfactory dysfunction. This lack of association could be attributed to the heterogeneity of factors potentially involved in the pathophysiology of these clinical symptoms. For example, olfactory dysfunction appears to be more directly linked to the effect of the virus on the olfactory epithelium during the acute stage, while fatigue is related to central, immunological, and peripheral mechanisms [49, 50]. The correlation observed between ChP and cognitive deficits underscores the specific role of the ChP in this context. In addition, these findings suggest the importance of individually analyzing each of the symptoms associated with PCC. This approach is relevant because several mechanisms, which are not mutually exclusive, may contribute to the generation of the clinical presentation.

Furthermore, ChP volume was also associated with brain structural and functional alterations. The ChP enlargement in PCC was related to WM integrity and diffusivity changes, specifically with reduced FA and increased AD. Enlarged ChP volume was associated with FA reduction in WM tracts located close to the ChP, including the Fornix, Callosal body, and Anterior thalamic radiation. Similarly, ChP volume was also related to increased AD in those tracts, but also in the Uncinate, Inferior Fronto-occipital, and Middle Longitudinal tracts, which connect with the frontal and temporal lobes. These alterations were related mostly with attention and memory deficits in PCC. WM alterations have previously been described in PCC showing altered WM integrity and diffusivity [13].

These structural alterations were accompanied by FC alterations. ChP volume also revealed associations with increased FC between subcortical, frontal, temporal, and cerebellar areas. Specifically, reduced ChP volume was associated with increased FC between caudate and orbitofrontal areas, and between frontal and posterior cingulate, and cerebellar areas. Worth to highlight, these FC alterations are spatially overlapped with GM volume alterations. Previous FC studies in PCC also found FC alterations [14, 51].

The immunological analysis also revealed significant findings, showing associations with the ChP, which links the periphery with the central nervous system through the ChP. The increased ChP volume in PCC patients was associated with reduced $CD11b^{+}$ expression and increased expression of CX3CR1. Interestingly, some studies report CX3CR1 to have good accuracy for classifying disease severity [52]. In addition, PCC patients presented with reduced proportion of $CD14^{+}CD16^{+}$ monocytes and CCR2 compared to HC. These findings could suggest a potential recruitment of intermediate monocytes from peripheral blood to the ChP in these patients, exacerbating inflammation. Moreover, these alterations may be more accentuated in ChP-large subgroup compared to ChP-small, showing lower proportion of $CD11b^{+}$ and CCR5, but increased expression of CD69. These findings imply a possible migration of pro-inflammatory monocytes through an increased expression of $CD11b^{+}$ from the bloodstream to the central nervous system, aligning with the hypothesis of recruitment towards pro-inflammatory stimuli within the ChP. Changes in intermediate monocytes have been previously reported in convalescent COVID-19 individuals, presenting with lower circulating intermediate monocytes [53].

The ChP volume enlargement has been suggested to be related to changes in permeability, which could include increased flow of toxic substances into the cerebrospinal fluid, and/or a decreased flow of the essential nutrients from the blood into the cerebrospinal fluid [45]. Specifically, a recent study found increased ChP volume and reduced permeability in Alzheimer's disease subgroup compared to mild cognitive impairment subgroup [45], suggesting that neuroinflammation could increase permeability in early stages but be reduced as the disease progresses to degeneration [54]. Another study negatively related the ChP volume with levels of CSF protein [55]. Moreover, ChP volume has been inversely related to clearance of the CSF [56]. Therefore, these previous evidences linked to the present findings raise the hypothesis that when the ChP enlargement reaches a certain volume, immune cells or toxins may enter the brain through the ChP-CSF system and are less prone to be removed, causing neuroinflammation, GM volume changes, and consequently, cognitive deficits. In fact, a previous study suggested that the sustained inflammation in COVID-19 could unchain the progressive loss of ChP function linked to microglial alterations and consequently, cognitive deterioration [57].

Overall, our findings may be interpreted in two main ways, which may indeed complement each other. Firstly, the ChP could be targeted during the acute infection due to its susceptibility to direct viral effects (because of the affinity of the virus for this structure) and indirect mechanisms (such as inflammation or hypoxia), which could be supported by recent findings showing enlarged ChP volume in subacute COVID-19 patients [27]. Secondly, the ChP could suffer damage during the post-acute stages due to persistent immune activation in the periphery. In this scenario, activated inflammatory cells might initiate inflammation in the brain barriers, potentially leading to anatomical and functional disruption of the ChP. The latter mechanism has been shown in multiple sclerosis, in which ChP volume is suggested as an imaging biomarker of inflammation and disease activity [58, 59]. Once the ChP is enlarged by either

mechanism, it may increase its permeability, allowing the passage of immune cells, cytokines, and/or other blood constituents causing neuroinflammation and brain damage. ChP has also an increasingly recognized role in the glymphatic system, a recently discovered brain extracellular clearance system, which may also be dysfunctional after SARS-CoV-2 infection [60]. These mechanisms set off a cascade of structural and functional changes in the brain, ultimately leading to cognitive impairment. Notably, brain regions correlated with ChP volumes are anatomically associated by the CSF or in close proximity, supporting the rationale for this mechanism of damage driven by the disruption of the blood-CSF barrier. Longitudinal studies are necessary at different time points since the acute infection to further understand the role of ChP and their potential use as an imaging biomarker of neuroinflammation in PCC.

Some limitations should be considered. First, our study has a cross-sectional design, with patients undergoing evaluation approximately at mean of 14 months after the infection and with no previous assessments. Second, the ChP segmentation might not be entirely accurate in delineating its complex structure. However, we used a validated algorithm that underwent visual checking by two independent researchers in a high-resolution 3D-T1 sequence [28]. The incorporation of additional neuroimaging methods, such as advanced T2 mapping techniques, may be of interest to inform about ChP pathology in future studies. Third, immunological analysis was conducted only in a subset of patients, focusing on the assessment of monocytes. Finally, we used standard and well-established DTI analysis techniques. However, some novel approaches (e.g., fixel-based analysis) may be of interest in future studies of white matter changes to prevent the limitations of crossing fiber areas [61].

In conclusion, results revealed that the ChP is enlarged in patients with PCC who report cognitive complaints. ChP volume was found to be correlated with cognitive performance, as well as structural and functional changes in the brain. This highlights a key role of ChP integrity in the pathophysiology of cognitive deficits and the observed brain changes in PCC. The previously documented function of the ChP in maintaining brain homeostasis and regulating the entry of immune cells into the brain supports the presence of neuroinflammatory mechanisms in this disorder.

DATA AVAILABILITY

The anonymized data will be provided in compliance with Health Research Institute "San Carlos" (IdISCC) from Hospital Clinico San Carlos, available from the corresponding author upon reasonable request. Requests for the data should be submitted to JAMG.

REFERENCES

1. Soriano JB, Murthy S, Marshall JC, Relan P, Diaz JV. A clinical case definition of post-COVID-19 condition by a Delphi consensus. Lancet Infect Dis. 2022;22:e102–7.
2. Premraj L, Kannapadi NV, Briggs J, Seal SM, Battaglini D, Fanning J, et al. Mid and long-term neurological and neuropsychiatric manifestations of post-COVID-19 syndrome: a meta-analysis. J Neurol Sci. 2022;434:120162.
3. Zhao S, Martin EM, Reuken PA, Scholcz A, Ganse-Dumrath A, Srowig A, et al. Long COVID is associated with severe cognitive slowing: a multicentre cross-sectional study. EClinicalMedicine. 2024;68. https://doi.org/10.1016/j.eclinm.2024.102434.
4. Hampshire A, Azor A, Atchison C, Trender W, Hellyer PJ, Giunchiglia V, et al. Cognition and memory after Covid-19 in a large community sample. N. Engl J Med. 2024;390:806–18. https://doi.org/10.1056/NEJMoa2311330.
5. Nicotra A, Masserini F, Calcaterra F, Di Vito C, Doneddu PE, Pomati S, et al. What do we mean by long COVID? A scoping review of the cognitive sequelae of SARS-CoV-2 infection. Eur J Neurol [Internet]. 2023;30:3968–78. https://doi.org/10.1111/ene.16027.
6. Delgado-Alonso C, Cuevas C, Oliver-Mas S, Díez-Cirarda M, Delgado-Álvarez A, Gil-Moreno MJ, et al. Fatigue and Cognitive Dysfunction Are Associated with Occupational Status in Post-COVID Syndrome. Vol. 19, International Journal of Environmental Research and Public Health. 2022.
7. Mohammadi S, Ghaderi S Post-COVID-19 conditions: a systematic review on advanced magnetic resonance neuroimaging findings. Neurol Sci. 2024. https://doi.org/10.1007/s10072-024-07427-6.
8. Petersen M, Nägele FL, Mayer C, Schell M, Petersen E, Kühn S, et al. Brain imaging and neuropsychological assessment of individuals recovered from a mild to moderate SARS-CoV-2 infection. Proc Natl Acad Sci [Internet]. 2023;120:e2217232120 https://doi.org/10.1073/pnas.2217232120.
9. Zhao S, Toniolo S, Hampshire A, Husain M. Effects of COVID-19 on cognition and brain health. Trends Cogn Sci. 2023;27:1053–67. https://doi.org/10.1016/j.tics.2023.08.008.
10. Díez-Cirarda M, Yus M, Gómez-Ruiz N, Polidura C, Gil-Martínez L, Delgado-Alonso C, et al. Multimodal neuroimaging in post-COVID syndrome and correlation with cognition. Brain. 2022;awac384. https://doi.org/10.1093/brain/awac384.
11. Douaud G, Lee S, Alfaro-Almagro F, Arthofer C, Wang C, McCarthy P, et al. SARS-CoV-2 is associated with changes in brain structure in UK Biobank. Nature. 2022;604:697–707. https://doi.org/10.1038/s41586-022-04569-5.
12. Huang S, Zhou Z, Yang D, Zhao W, Zeng M, Xie X, et al. Persistent white matter changes in recovered COVID-19 patients at the 1-year follow-up. Brain. 2021;145:1830–8.
13. Boito D, Eklund A, Tisell A, Levi R, Özarslan E, Blystad I. MRI with generalized diffusion encoding reveals damaged white matter in patients previously hospitalized for COVID-19 and with persisting symptoms at follow-up. Brain Commun. 2023;5:fcad284 https://doi.org/10.1093/braincomms/fcad284.
14. Voruz P, Cionca A, Jacot de Alcântara I, Nuber-Champier A, Allali G, Benzakour L, et al. Brain functional connectivity alterations associated with neuropsychological performance 6–9 months following SARS-CoV-2 infection. Hum Brain Mapp. 2023;44:1629–46. https://doi.org/10.1002/hbm.26163.
15. Fernández-Castañeda A, Lu P, Geraghty AC, Song E, Lee MH, Wood J, et al. Mild respiratory COVID can cause multi-lineage neural cell and myelin dysregulation. Cell 2022;185:2452–.e16.
16. Monje M, Iwasaki A. The neurobiology of long COVID. Neuron. 2022;110:3484–96.
17. Matschke J, Lütgehetmann M, Hagel C, Sperhake JP, Schröder AS, Edler C, et al. Neuropathology of patients with COVID-19 in Germany: a post-mortem case series. Lancet Neurol. 2020;19:919–29. https://doi.org/10.1016/S1474-4422(20)30308-2.
18. Talhada D, Costa-Brito AR, Duarte AC, Costa AR, Quintela T, Tomás J, et al. The choroid plexus: simple structure, complex functions. J Neurosci Res. 2020;98:751–3. https://doi.org/10.1002/jnr.24571.
19. Ghersi-Egea JF, Strazielle N, Catala M, Silva-Vargas V, Doetsch F, Engelhardt B. Molecular anatomy and functions of the choroidal blood-cerebrospinal fluid barrier in health and disease. Acta Neuropathol. 2018;135:337–61. https://doi.org/10.1007/s00401-018-1807-1.
20. Greene C, Connolly R, Brennan D, Laffan A, O'Keeffe E, Zaporojan L, et al. Blood–brain barrier disruption and sustained systemic inflammation in individuals with long COVID-associated cognitive impairment. Nat Neurosci. 2024. https://doi.org/10.1038/s41593-024-01576-9.
21. Pellegrini L, Albecka A, Mallery DL, Kellner MJ, Paul D, Carter AP, et al. SARS-CoV-2 infects the brain choroid plexus and disrupts the blood-CSF barrier in human brain organoids. Cell Stem Cell. 2020;27:951–.e5. https://doi.org/10.1016/j.stem.2020.10.001.
22. Jacob F, Pather SR, Huang WK, Zhang F, Wong SZH, Zhou H, et al. Human pluripotent stem cell-derived neural cells and brain organoids reveal SARS-CoV-2 neurotropism predominates in choroid plexus epithelium. Cell Stem Cell. 2020;27:937–.e9. https://doi.org/10.1016/j.stem.2020.09.016.
23. Yang AC, Kern F, Losada PM, Agam MR, Maat CA, Schmartz GP, et al. Dysregulation of brain and choroid plexus cell types in severe COVID-19. Nature. 2021;595:565–71. https://doi.org/10.1038/s41586-021-03710-0.
24. Fleischer V, Gonzalez-Escamilla G, Ciolac D, Albrecht P, Küry P, Gruchot J, et al. Translational value of choroid plexus imaging for tracking neuroinflammation in mice and humans. Proc Natl Acad Sci. 2021;118:e2025000118 https://doi.org/10.1073/pnas.2025000118.
25. Ricigliano VAG, Morena E, Colombi A, Tonietto M, Hamzaoui M, Poirion E, et al. Choroid plexus enlargement in inflammatory multiple sclerosis: 3.0-T MRI and translocator protein PET evaluation. Radiology. 2021;301:166–77. https://doi.org/10.1148/radiol.2021204426.
26. Assogna M, Premi E, Gazzina S, Benussi A, Ashton NJ, Zetterberg H, et al. Association of choroid plexus volume with serum biomarkers, clinical features, and disease severity in patients with frontotemporal lobar degeneration spectrum. Neurology. 2023;101:e1218–30. https://doi.org/10.1212/WNL.0000000000207600.
27. Rau A, Gonzalez-Escamilla G, Schroeter N, Othman A, Dressing A, Weiller C, et al. Inflammation-triggered enlargement of choroid plexus in subacute COVID-19 patients with neurological symptoms. Ann Neurol 2024;96:715–25. https://doi.org/10.1002/ana.27016.
28. Tadayon E, Moret B, Sprugnoli G, Monti L, Pascual-Leone A, Santarnecchi E, et al. Improving choroid plexus segmentation in the healthy and diseased brain: relevance for Tau-PET imaging in dementia. J Alzheimer's Dis. 2020;74:1057–68.
29. Ashburner J, Barnes G, Chen CC, Daunizeau J, Flandin G, Friston K, et al. SPM12 manual. Wellcome Trust Centre for Neuroimaging: London, UK; 2014. 2464, 4.
30. Fischl B. FreeSurfer. Neuroimage. 2012;62:774–81.
31. Fischl B, Sereno MI, Dale AM. Cortical surface-based analysis: II: inflation, flattening, and a surface-based coordinate system. Neuroimage. 1999;9:195–207.

32. Dale AM, Fischl B, Sereno MI. Cortical surface-based analysis: I. Segmentation and surface reconstruction. Neuroimage. 1999;9:179–94.
33. Fischl B, Salat DH, Busa E, Albert M, Dieterich M, Haselgrove C, et al. Whole brain segmentation: automated labeling of neuroanatomical structures in the human brain. Neuron. 2002;33:341–55. https://doi.org/10.1016/S0896-6273(02)00569-X.
34. Smith SM, Jenkinson M, Woolrich MW, Beckmann CF, Behrens TEJ, Johansen-Berg H, et al. Advances in functional and structural MR image analysis and implementation as FSL. Neuroimage. 2004;23:S208–19.
35. Andersson JLR, Skare S, Ashburner J. How to correct susceptibility distortions in spin-echo echo-planar images: application to diffusion tensor imaging. Neuroimage. 2003;20:870–88.
36. Smith SM. Fast robust automated brain extraction. Hum Brain Mapp. 2002;17:143–55. https://doi.org/10.1002/hbm.10062.
37. Andersson JLR, Sotiropoulos SN. An integrated approach to correction for off-resonance effects and subject movement in diffusion MR imaging. Neuroimage. 2016;125:1063–78.
38. Smith SM, Jenkinson M, Johansen-Berg H, Rueckert D, Nichols TE, Mackay CE, et al. Tract-based spatial statistics: voxelwise analysis of multi-subject diffusion data. Neuroimage. 2006;31:1487–505.
39. Whitfield-Gabrieli S, Nieto-Castanon A. Conn: a functional connectivity toolbox for correlated and anticorrelated brain networks. Brain Connect. 2012;2:125–41.
40. Xia M, Wang J, He Y. BrainNet viewer: a network visualization tool for human brain connectomics. PLoS One. 2013;8:e68910 https://doi.org/10.1371/journal.pone.0068910.
41. Wong KL, Yeap WH, Tai JJY, Ong SM, Dang TM, Wong SC. The three human monocyte subsets: implications for health and disease. Immunol Res. 2012;53:41–57. https://doi.org/10.1007/s12026-012-8297-3.
42. Hayes AF. Introduction to mediation, moderation, and conditional process analysis: a regression-based approach. Guilford Publications; 2017.
43. Field A Discovering statistics using IBM SPSS statistics. sage; 2013.
44. Hojat M, Xu G. A visitor's guide to effect sizes–statistical significance versus practical (clinical) importance of research findings. Adv Health Sci Educ. 2004;9:241–9.
45. Choi JD, Moon Y, Kim HJ, Yim Y, Lee S, Moon WJ. Choroid plexus volume and permeability at brain MRI within the Alzheimer disease clinical spectrum. Radiology. 2022;304:635–45. https://doi.org/10.1148/radiol.212400.
46. Heine J, Schwichtenberg K, Hartung TJ, Rekers S, Chien C, Boesl F, et al. Structural brain changes in patients with post-COVID fatigue: a prospective observational study. EClinicalMedicine. 2023;58. https://doi.org/10.1016/j.eclinm.2023.101874.
47. Zorzo C, Solares L, Mendez M, Mendez-Lopez M. Hippocampal alterations after SARS-CoV-2 infection: a systematic review. Behavioural Brain Res. 2023;455:114662.
48. Díez-Cirarda M, Yus-Fuertes M, Sanchez-Sanchez R, Gonzalez-Rosa JJ, Gonzalez-Escamilla G, Gil-Martínez L, et al. Hippocampal subfield abnormalities and biomarkers of pathologic brain changes: from SARS-CoV-2 acute infection to post-COVID syndrome. EBioMedicine. 2023;94:104711
49. Al-Hakeim HK, Al-Rubaye HT, Al-Hadrawi DS, Almulla AF, Maes M. Long-COVID post-viral chronic fatigue and affective symptoms are associated with oxidative damage, lowered antioxidant defenses and inflammation: a proof of concept and mechanism study. Mol Psychiatry. 2023;28:564–78. https://doi.org/10.1038/s41380-022-01836-9.
50. Butowt R, Bilinska K, von Bartheld CS. Olfactory dysfunction in COVID-19: new insights into the underlying mechanisms. Trends Neurosci. 2023;46:75–90.
51. Goehringer F, Bruyere A, Doyen M, Bevilacqua S, Charmillon A, Heyer S, et al. Brain 18F-FDG PET imaging in outpatients with post-COVID-19 conditions: findings and associations with clinical characteristics. Eur J Nucl Med Mol Imaging. 2022. https://doi.org/10.1007/s00259-022-06013-2.
52. Maucourant C, Filipovic I, Ponzetta A, Aleman S, Cornillet M, Hertwig L, et al. Natural killer cell immunotypes related to COVID-19 disease severity. Sci Immunol. 2020;5:eabd6832.
53. Ravkov EV, Williams ESCP, Elgort M, Barker AP, Planelles V, Spivak AM, et al. Reduced monocyte proportions and responsiveness in convalescent COVID-19 patients. Front Immunol. 2024;14. https://www.frontiersin.org/journals/immunology/articles/10.3389/fimmu.2023.1329026.
54. Chiang GC. The blood–cerebrospinal fluid barrier may play a role in Alzheimer disease pathogenesis. Radiology. 2022;304:646–7. https://doi.org/10.1148/radiol.220740.
55. Tadayon E, Pascual-Leone A, Press D, Santarnecchi E. Choroid plexus volume is associated with levels of CSF proteins: relevance for Alzheimer's and Parkinson's disease. Neurobiol Aging. 2020;89:108–17.
56. Althubaity N, Schubert J, Martins D, Yousaf T, Nettis MA, Mondelli V, et al. Choroid plexus enlargement is associated with neuroinflammation and reduction of blood brain barrier permeability in depression. Neuroimage Clin. 2022;33:102926
57. Suzzi S, Tsitsou-Kampeli A, Schwartz M. The type I interferon antiviral response in the choroid plexus and the cognitive risk in COVID-19. Nat Immunol. 2023;24:220–4. https://doi.org/10.1038/s41590-022-01410-z.
58. Muthuraman M, Oshaghi M, Fleischer V, Ciolac D, Othman A, Meuth SG, et al. Choroid plexus imaging to track neuroinflammation – a translational model for mouse and human studies. Neural Regen Res. 2023;18. https://journals.lww.com/nrronline/fulltext/2023/03000/choroid_plexus_imaging_to_track_neuroinflammation.12.aspx.
59. Bergsland N, Dwyer MG, Jakimovski D, Tavazzi E, Benedict RHB, Weinstock-Guttman B, et al. Association of choroid plexus inflammation on MRI with clinical disability progression over 5 years in patients with multiple sclerosis. Neurology. 2023;100:e911–20. https://doi.org/10.1212/WNL.0000000000201608.
60. Wu L, Zhang Z, Liang X, Wang Y, Cao Y, Li M, et al. Glymphatic system dysfunction in recovered patients with mild COVID-19: a DTI-ALPS study. iScience. 2024;27. https://doi.org/10.1016/j.isci.2023.108647.
61. Dhollander T, Clemente A, Singh M, Boonstra F, Civier O, Duque JD, et al. Fixel-based analysis of diffusion MRI: methods, applications, challenges and opportunities. Neuroimage. 2021;241:118417

ACKNOWLEDGEMENTS

This research has received funding from the Nominative Grant FIBHCSC 2020 COVID-19 (Department of Health, Community of Madrid). Jordi A. Matias-Guiu is supported by Instituto de Salud Carlos III through the project INT20/00079 and INT23/00017 (co-funded by European Regional Development Fund "A way to make Europe") and Fundación para el Conocimiento madri+d through the project G63-HEALTHSTARPLUS-HSP4. Maria Diez-Cirarda is supported by Instituto de Salud Carlos III (ISCIII) through Sara Borrell postdoctoral fellowship (Grant No. CD22/00043) and co-funded by the European Union. Gabriel Gonzalez-Escamilla is supported by the German research foundation (Deutsche Forschungsgemeinschaft (DFG); Radiomics SPP 2177, grant GO 3493/1-1). We would like to thank all the participants involved in the study.

AUTHOR CONTRIBUTIONS

The study design and administration were performed by MDC, JMG, GGE, JAMG. Recruitment was performed by CDA, MJGM, JAMG. Data Curation was carried out by MYF, LGM, CDA, MJGM, SSR, CJG, SOM, NGR, CP, MJ, JA, UGP, JAMG. The analyses were performed by MDC, MYF, LGM, SSR, CJG, JAMG. Investigation and interpretation of data were performed by all authors. Visualization of results was performed by MDC, JAMG. Whole process was supervised by MDC, GGE, JAMG. MDC, GGE, JAMG, CJG, SSR wrote the first draft. All authors reviewed and edited the manuscript. All authors have confirmed that they had full access to all the data in the study and accept responsibility to submit for publication.

COMPETING INTERESTS

The authors declare no competing interests.

ADDITIONAL INFORMATION

Supplementary information The online version contains supplementary material available at https://doi.org/10.1038/s41380-024-02886-x.

Correspondence and requests for materials should be addressed to Maria Diez-Cirarda or Jordi A. Matias-Guiu.